NANO LETTERS

Letter

pubs.acs.org/NanoLett

A Thermally Conductive Separator for Stable Li Metal Anodes

Wei Luo,[†,‡] Lihui Zhou,[†] Kun Fu,[†] Zhi Yang,[‡] Jiayu Wan,[†] Michael Manno,[‡] Yonggang Yao,[†] Hongli Zhu,[†] Bao Yang,[*,‡] and Liangbing Hu[*,†]

[†]Department of Materials Science and Engineering and [‡]Department of Mechanical Engineering, University of Maryland, College Park, Maryland 20742, United States

Supporting Information

ABSTRACT: Li metal anodes have attracted considerable research interest due to their low redox potential (−3.04 V vs standard hydrogen electrode) and high theoretical gravimetric capacity of 3861 mAh/g. Battery technologies using Li metal anodes have shown much higher energy density than current Li-ion batteries (LIBs) such as Li−O_2 and Li−S systems. However, issues related to dendritic Li formation and low Coulombic efficiency have prevented the use of Li metal anode technology in many practical applications. In this paper, a thermally conductive separator coated with boron-nitride (BN) nanosheets has been developed to improve the stability of the Li metal anodes. It is found that using the BN-coated separator in a conventional organic carbonate-based electrolyte results in the Coulombic efficiency stabilizing at 92% over 100 cycles at a current rate of 0.5 mA/cm^2 and 88% at 1.0 mA/cm^2. The improved Coulombic efficiency and reliability of the Li metal anodes is due to the more homogeneous thermal distribution resulting from the thermally conductive BN coating and to the smaller surface area of initial Li deposition.

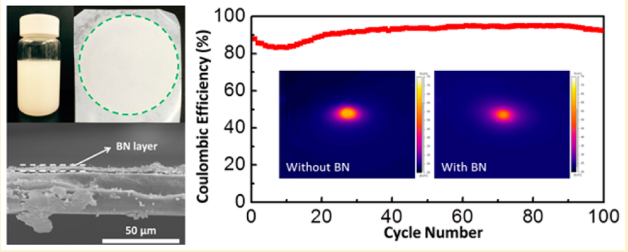

KEYWORDS: *Li metal anode, Coulombic efficiency, BN nanosheets, thermally conductive separator, uniform thermal distribution*

Lithium-ion batteries (LIBs) have been critical for powering portable electronics since their commercialization in early 1990s.[1] To meet the ever-increasing demands of new electric vehicles and electrical energy storage for renewable energy resources, LIBs with high energy density are required. Unfortunately, graphite-based anode employed in current LIB system exhibits a low specific capacity, significantly limiting the energy density of LIBs. Therefore, significant effort has been focused on developing anodes with high specific capacity, such as Si[2−5] and Li metal.[6−8] Alternative battery technologies, such as Li−S[9−13] and Li−O_2 batteries[14−17] have attracted considerable attentions because of their high energy densities, and although they consist of different chemistries, Li−S and Li−O_2 systems utilize the same Li metal anode due to its low redox potential (−3.04 V vs standard hydrogen electrode) and high theoretical gravimetric capacity of 3861 mAh/g. However, issues associated with Li metal anodes, including uncontrollable dendritic Li growth and low Coulombic efficiency upon electrochemical cycling, have impeded their use in practical application. With the urgent demand of high-energy-density batteries, developing safe and stable Li metal anodes has become very pivotal but remains a significant challenge to chemists and materials scientists.

In order to address the issues found in Li metal anodes, many approaches have been explored. To inhibit the dendritic Li growth, some researchers exploited a uniform and stable solid electrolyte interphase (SEI) layer on Li metal surface, which is used to adjust the components and additives of liquid electrolyte.[18−22] For example, Xu and Zhang reported that $CsPF_6$ additive can effectively enhance the stability of SEI and thus suppress the dendritic Li growth.[23,24] An alternative approach using solid or gel electrolyte to improve mechanical strength and operational lifetime has also been studied.[25−29] Most recently, Cui and co-workers developed a promising approach based on designing and fabricating stable interfacial nanomaterials, like a monolayer of interconnected amorphous hollow carbon spheres[30] and two-dimensional (2D) atomic crystal layers.[31] These interfacial nanomaterials can effectively afford a protection for Li metal anode during electrochemical cycling, which leads to stable cycling performance.

In addition to the work on electrolyte additives, solid-state electrolytes, and interfacial materials, modifying the separator has also been studied as a method to achieve stable Li metal anodes.[32−35] In previous research, different ceramic and organic materials were used to coat a commercial separator.[36−40] In this study, we propose a novel boron nitride (BN) nanosheet coated separator for stable Li metal anodes. In a typical commercial separator (Figure 1a), Li wires are grown on the current collector during initial Li deposition. The Li wires consume a large number of electrolytes due to their large surface area, resulting in low Coulombic efficiency and eventual growth of dendritic Li.[6] As shown in Figure 1b, we hypothesize that a thermally conductive BN coating can result in a uniform

Received: June 19, 2015
Revised: July 25, 2015
Published: August 3, 2015

DOI: 10.1021/acs.nanolett.5b02432
Nano Lett. 2015, 15, 6149−6154

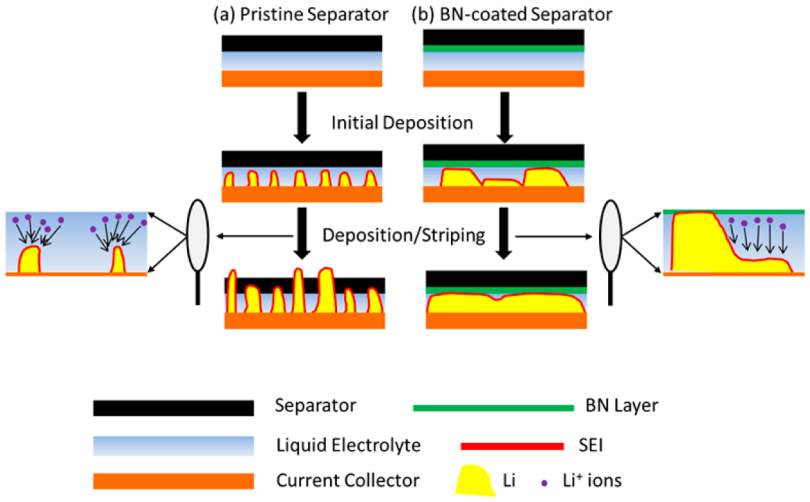

Figure 1. Schematic of Li deposition/striping process with pristine separator and BN-coated separator: (a) repeated Li deposition/striping cycles lead to the growth of dendritic Li; (b) BN coating leads to a uniform deposition/striping of Li.

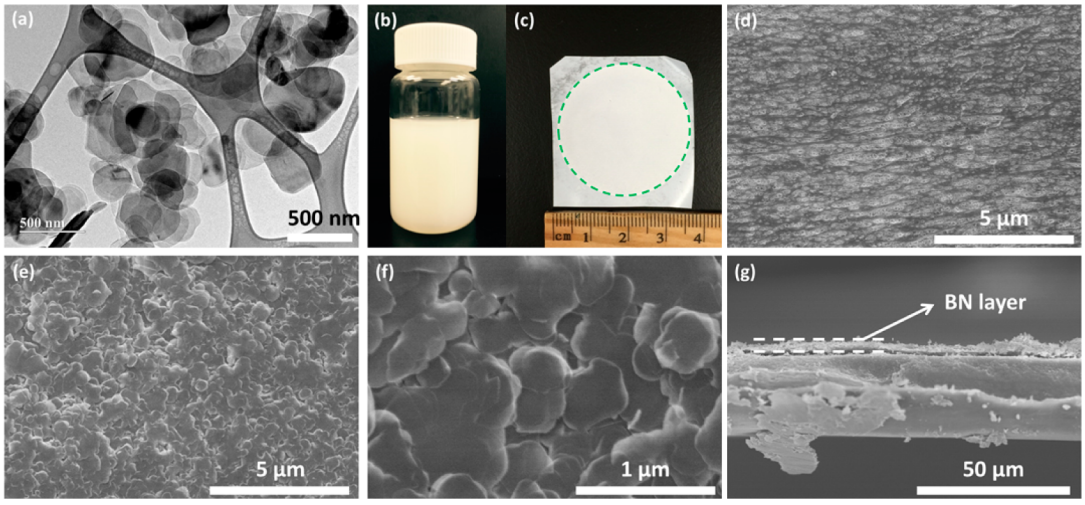

Figure 2. (a) A TEM image of BN nanosheets. Digital images of (b) BN/PVDF/NMP suspension and (c) BN-coated separator (BN layer is marked by green circle). SEM images of (d) pristine separator, (e, f) top view, and (g) cross-section view of BN-coated separator.

deposition/striping of Li due to the smaller total surface area of the initial deposited Li wires and a more homogeneous thermal distribution, decreasing the risk of dendritic Li growth and improving cycling performance.

Results and Discussion. Hexagonal boron nitride, also known as "white graphene", is one of the most studied 2D materials due to its chemical stability, electrical insulation, and very high thermal conductivity.[41−43] BN bulk powder, purchased from Sigma-Aldrich, exhibits a typical hexagonal phase (Figure S1a, Supporting Information) and flake morphology with a size of ∼500 nm (Figure S1b,c, Supporting Information). BN powder is exfoliated by a sonication procedure using *N*-methyl pyrrolidone (NMP) as the solvent.[44−46] After sonication, BN nanosheets are prepared, as clearly indicated by scanning electron microscopy (SEM) images (Figure S2a,b, Supporting Information). To give further insight into the microstructure of BN nanosheets, transmission electron microscopy (TEM) and atomic force microscopy (AFM) images are also taken. As shown in Figure 2a, the typical BN nanosheet is about 500 nm in diameter. The size of BN nanosheet is maintained well as its precursor, which is beneficial to get a uniform coating on the separator. Moreover, the BN layer would not cause shorting of batteries because BN is an electronic insulator. The typical thickness of BN nanosheet is ∼9.0 nm, as determined by AFM (Figure S2c, Supporting Information). Polyvinylidene fluoride (PVDF) binder is then added into the BN nanosheets/NMP suspension under sonication with a BN/PVDF mass ratio of 9:1. The as-prepared BN/PVDF/NMP suspension (Figure 2b) is coated onto one side of a commercial separator (Celgard 2325) by vacuum filtration followed by drying in a vacuum oven at 60 °C overnight. As marked by the green circle in Figure 2c, the surface of the separator becomes white and less specular after BN coating. As shown in Figure 2d, a large number of pores are observed in the surface of the pristine separator, and after coating, these pores are covered by BN nanosheets with a particle size of ∼500 nm (Figure 2e,f). The thickness of the BN layer is about 1 μm with a mass loading of ∼0.2 mg/cm^2 (Figure 2g), where the electrolyte uptake is slightly increased to 245% for BN-coated separator compared to pristine separator (180%).

To investigate the electrochemical performance, pristine and BN-coated separator are employed in Li/Cu cells,[30,31] where Cu foil is used as the working electrode, Li foil as the counter/

DOI: 10.1021/acs.nanolett.5b02432
Nano Lett. 2015, 15, 6149−6154

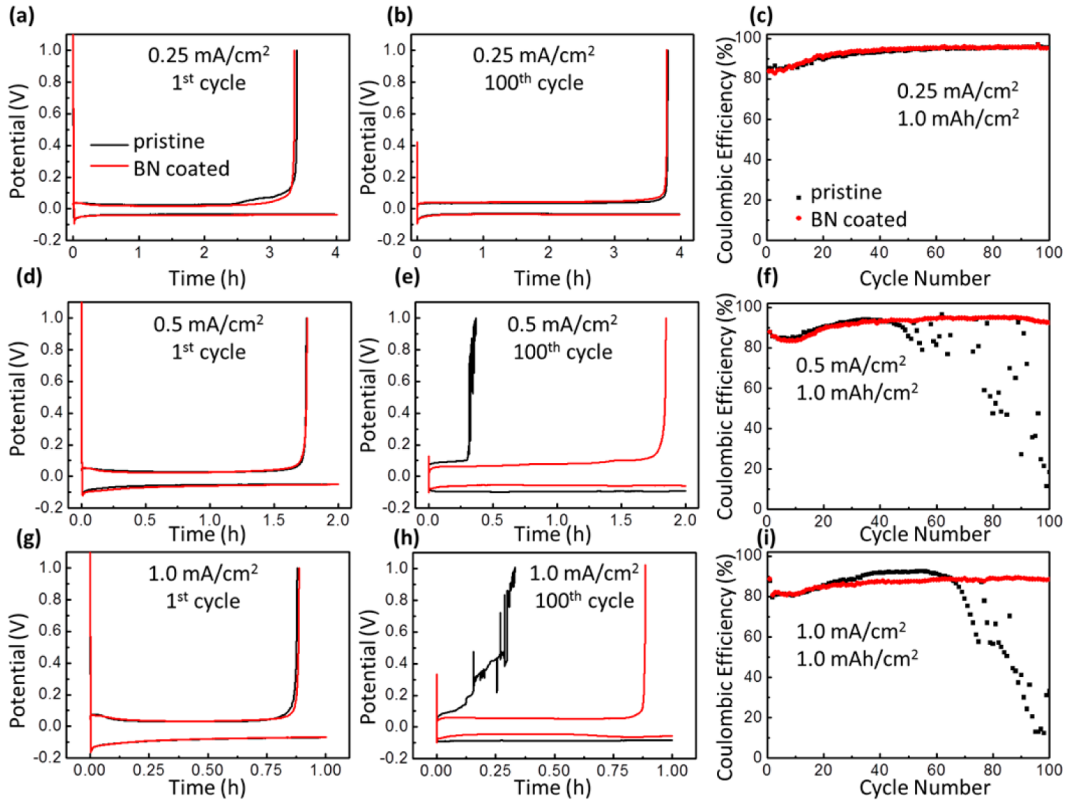

Figure 3. Electrochemical performance of Li/Cu cells with pristine separator (black) and BN-coated separator (red) at various current densities with a depostion capacity of 1.0 mAh/cm^2: potential profiles for the first and 100th cycle at (a, b) 0.25 mA/cm^2, (d, e) 0.5 mA/cm^2, and (g, h) 1.0 mA/cm^2; Coulombic efficiencies at (c) 0.25 mA/cm^2, (f) 0.5 mA/cm^2, and (i) 1.0 mA/cm^2.

reference electrode, and 1.0 M $LiPF_6$ in ethylene carbonate/diethyl carbonate (EC:DEC = 1:1 by volume) solution as the electrolyte. Li deposition/striping cycles between Cu working electrode and Li counter/reference electrode are performed at various current densities. The deposition capacity is set to be 1.0 mAh/cm^2, and the cutoff potential for striping is set to be 1.0 V. Figure 3a compares the potential profiles of cells at the first cycle with pristine separator and BN-coated separator under a current density of 0.25 mA/cm^2. It is clear that the voltage rapidly drops below 0.0 V vs Li^+/Li for both cells, showing that Li starts to deposit on Cu electrodes. A similar overpotential is observed at the beginning of the Li deposition process for both cells, indicating that the BN coating does not cause higher impedance, which is also proven by electrochemical impedance spectroscopy (EIS) measurement (Figure S3, Supporting Information). Moreover, after 100 deposition/striping cycles, the potential profiles of two cells still overlap each other very well (Figure 3b). The similar impedance and Coulombic efficiencies (Figure 3c) prove that Li metal anode works well at a small current density,[47] and the thin layer coating of BN nanosheets does not affect its performance at this condition.

Rate capability is also very important in practical applications that the current density is increased to 0.5 mA/cm^2 with a deposition time of 2 h. As shown in Figure 3d, the potential profile in the first cycle for the cell using pristine separator also overlaps that of cell with the BN-coated separator. However, after repeating deposition/striping for 50 cycles, the cell using pristine separator shows an unstable striping process, while the BN-coated separator cell still exhibits a stable striping profile (Figure S4, Supporting Information). Furthermore, the cell with pristine separator shows a very short striping process after 100 cycles, which sharply contrasts with the stable striping of the BN-coated separator cell (Figure 3e). The fast decay in deposition/striping process corresponds to the fact that Coulombic efficiency drops to 85% after 50 cycles and 18% after 100 cycles in the cell with pristine separator. In comparison, a stable Coulombic efficiency of ~92% after 100 cycles can be maintained with BN-coated separator (Figure 3f), and a similar result is also observed when the current density is further increased to 1.0 mA/cm^2. The cell with a BN-coated separator shows stable potential profiles and Coulombic efficiency maintains at 88% after 100 cycles, while the control experiment shows unstable potential profiles and decay in Coulombic efficiency (Figure 3g–i). The above observations demonstrate that the cycling performance of the Li metal anode at high current densities is significantly improved by using the BN-coated separator.

It is known that the morphology of the electrochemical Li deposition plays a critical role in Coulombic efficiency. Ex situ SEM observations are carried out on Cu working electrodes before and after Li deposition at a current density of 1.0 mA/cm^2 for 1 h. As shown in Figure 4c, a large number of one-dimensional (1D) Li wires are grown on Cu foil (Figure 4a and b) after Li deposition using pristine separator. When zooming in, we can found that these Li wires have a typical diameter of 200 nm (Figure 4d). Interestingly, the diameter of deposited Li wire becomes much larger when using BN-coated separator (Figure 4e and f). According to previous studies,[6,7] the larger diameter of Li wires can lead to a smaller total surface area, resulting in less contact between the electrode and electrolyte and less consumption of electrolyte. The smaller total surface

DOI: 10.1021/acs.nanolett.5b02432
Nano Lett. 2015, 15, 6149–6154

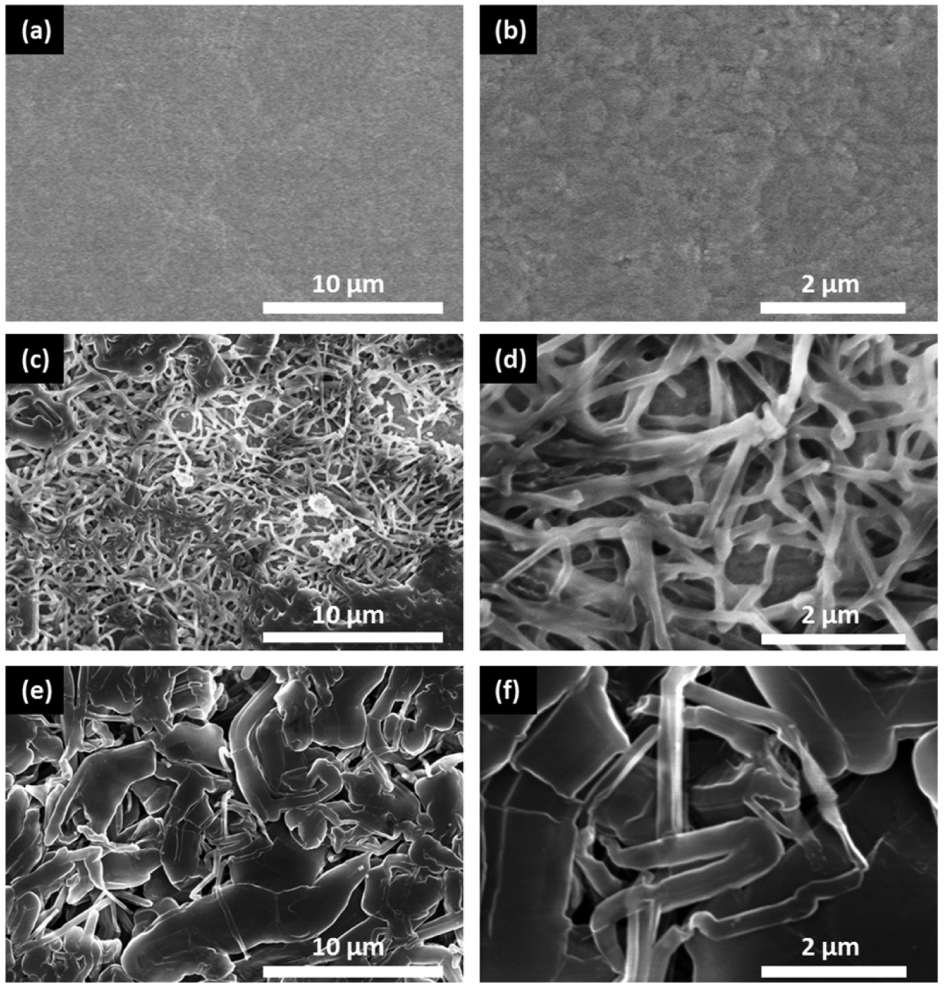

Figure 4. Morphology observation for electrochemical Li deposition. SEM images of (a, b) pristine Cu foil, Li deposition on Cu foil at current density of 1.0 mA/cm^2 for 1 h with (c, d) pristine separator and (e, f) BN-coated separator.

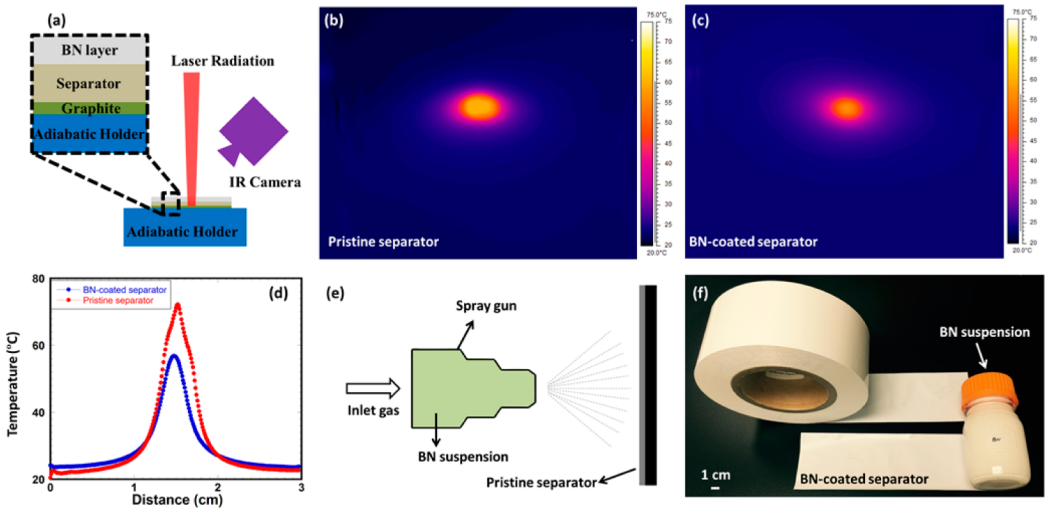

Figure 5. (a) Schematic illustration of mapping the temperature distribution when a hotspot is created on the separators by a focused laser beam; (b, c) temperature distribution images and (d) corresponding temperature lines on pristine separator and BN-coated separator; (e) schematic of producing BN-coated separator by spray coating technology; (f) an image of BN-coated separator fabricated by spray coating.

area also gives rise to a better cycling performance, which is consistent with the electrochemical results (Figure 3).

Here, we propose the following mechanism for the enhanced performance raised by using BN-coated separator. When Li is initiated to deposit on Cu working electrode with pristine separator, a large quantity of nuclei are formed, and subsequently Li wires with small diameter are grown around these nuclei after continuous deposition.[23] In contrast, with

DOI: 10.1021/acs.nanolett.5b02432
Nano Lett. 2015, 15, 6149−6154

BN-coated separator, less nuclei are formed, while Li^+ ions pass through the junctions between BN nanosheets on the separator. The diameter of deposited Li wires is much larger than that of the cell using pristine separator due to the fewer nuclei. Interestingly, our result is very similar to that Li grains can be capped underneath BN sheets in previous work.[31] The larger diameter of Li wires leads to a smaller surface area, and thus fewer electrolytes are consumed. On the other hand, as demonstrated by Xu and Zhang, a homogeneous electrical atmosphere is very important for uniform Li deposition/striping.[23,24] Here we propose that a homogeneous thermal atmosphere is also critical due to its exothermal nature during electrochemical reactions.[6] Unfortunately, the commercial separator is a poor thermally conductive material. For example, the polypropylene/polyethylene based separator exhibits a low thermal conductivity, < 1.0 W/m K. In contrast, the BN-coating on the polypropylene/polyethylene separator has a high thermal conductivity of 82 W/m K (Figure S5, detailed measurement is described in Supporting Information), which enhances the temperature uniformity during Li deposition/striping. To demonstrate the effects of the enhanced thermal conductivity, an infrared camera is used to map the temperature distribution when a hotspot is created on the separators by a focused laser beam (Figure 5a, detailed measurement is described in Supporting Information). As shown in Figure 5, the temperature spike is about 50 °C at the hotspot in the pristine separator. In comparison, the temperature spike is reduced to 34 °C due to the enhanced heat spreading with the BN nanosheets coating. It can be seen that the BN-coated separator can create a more uniform thermal distribution during Li deposition/striping cycling, which would lead to a more uniform growth/dissolution of Li and thus a better Coulombic efficiency and cycling performance.

It should be noted that the Coulombic efficiency obtained in this work is still not high enough. As reported previously, ionic liquid based electrolytes, adding additives into the electrolyte, or using ALD technology can improve the cycling performance.[20−22,48,49] However, to demonstrate the advantages of BN-coated separator, common $LiPF_6$-EC-DEC electrolyte is used in the study. We believe that performance can be further enhanced by combining other advanced technologies with the BN-coated separator and for large-scale production of BN-coated separator, spray coating technology can be used. Figure 5e shows a schematic of the spray coating, where the BN/PVDF suspension is loaded in the spray gun and deposited onto separator via a carrier gas (N_2). As shown in Figure 5f, a BN-coated separator with a length of 200 mm and width of 60 mm is successfully fabricated with this setup. Moreover, the commercial separator is produced on a roll (Figure 5f), which can be further coated with well-developed roll-to-roll technologies and thus shows great potential for practical applications.

Conclusion. In summary, an effective approach for improving the cycling stability of Li metal anode via a facile coating of commercial separator with a thermally conductive BN nanosheets was presented. When a deposition capacity of 1.0 mAh/cm^2 is applied in Li/Cu systems with common organic carbonate electrolyte ($LiPF_6$ in EC-DEC), the Coulombic efficiency can be maintained at 92% after 100 cycles at 0.5 mA/cm^2 and 88% after 100 cycles at 1.0 mA/cm^2 using BN-coated separator, while the Coulombic efficiency decays rapidly using a pristine separator at the same conditions. We find that initial Li deposition with a smaller surface area and a more homogeneous thermal atmosphere is important for Li deposition/striping and the stability of Li metal anodes. Considering that Li metal anodes are very promising for high-energy-density batteries, the concept of using a thermally conductive separator can shed light on further research. Moreover, by combining spray coating or other roll-to-roll technologies, the thermally conductive separator could be realized in practical applications.

■ ASSOCIATED CONTENT

Supporting Information

The Supporting Information is available free of charge on the ACS Publications website at DOI: 10.1021/acs.nanolett.5b02432.

Experimental section, characterization details, and supporting data (PDF)

■ AUTHOR INFORMATION

Corresponding Authors

*E-mail: binghu@umd.edu.

*E-mail: baoyang@umd.edu.

Notes

The authors declare no competing financial interest.

■ ACKNOWLEDGMENTS

The project is funded by the office of Naval research under grant N000141410721. The authors acknowledge the support of the Maryland Nanocenter and its Fablab, Nisplab, and surface analysis center. We also acknowledge Yanan Chen, Fei Shen, Hao Lin, Emily Hitz, and Dr. Xiaogang Han for their kind help in experiments.

■ REFERENCES

(1) Tarascon, J. M.; Armand, M. *Nature* **2001**, *414*, 359−367.

(2) Wu, H.; Cui, Y. *Nano Today* **2012**, *7*, 414−429.

(3) Liu, N.; Wu, H.; McDowell, M. T.; Yao, Y.; Wang, C.; Cui, Y. *Nano Lett.* **2012**, *12*, 3315−3321.

(4) Fu, K.; Yildiz, O.; Bhanushali, H.; Wang, Y.; Stano, K.; Xue, L.; Zhang, X.; Bradford, P. D. *Adv. Mater.* **2013**, *25*, 5109−5114.

(5) Liu, N.; Lu, Z.; Zhao, J.; McDowell, M. T.; Lee, H.-W.; Zhao, W.; Cui, Y. *Nat. Nanotechnol.* **2014**, *9*, 187−192.

(6) Xu, W.; Wang, J.; Ding, F.; Chen, X.; Nasybulin, E.; Zhang, Y.; Zhang, J.-G. *Energy Environ. Sci.* **2014**, *7*, 513−537.

(7) Ji, X.; Liu, D.-Y.; Prendiville, D. G.; Zhang, Y.; Liu, X.; Stucky, G. D. *Nano Today* **2012**, *7*, 10−20.

(8) Lu, D.; Shao, Y.; Lozano, T.; Bennett, W. D.; Graff, G. L.; Polzin, B.; Zhang, J.; Engelhard, M. H.; Saenz, N. T.; Henderson, W. A.; Bhattacharya, P.; Liu, J.; Xiao, J. *Adv. Energy Mater.* **2015**, *5*, 1400993.

(9) Ji, X.; Lee, K. T.; Nazar, L. F. *Nat. Mater.* **2009**, *8*, 500−506.

(10) Yang, Y.; Zheng, G.; Cui, Y. *Chem. Soc. Rev.* **2013**, *42*, 3018−3032.

(11) Zheng, G.; Yang, Y.; Cha, J. J.; Hong, S. S.; Cui, Y. *Nano Lett.* **2011**, *11*, 4462−4467.

(12) Li, Z.; Jiang, Y.; Yuan, L.; Yi, Z.; Wu, C.; Liu, Y.; Strasser, P.; Huang, Y. *ACS Nano* **2014**, *8*, 9295−9303.

(13) Ji, X.; Nazar, L. F. *J. Mater. Chem.* **2010**, *20*, 9821−9826.

(14) Bruce, P. G.; Freunberger, S. A.; Hardwick, L. J.; Tarascon, J.-M. *Nat. Mater.* **2012**, *11*, 19−29.

(15) Xiao, J.; Mei, D.; Li, X.; Xu, W.; Wang, D.; Graff, G. L.; Bennett, W. D.; Nie, Z.; Saraf, L. V.; Aksay, I. A.; Liu, J.; Zhang, J.-G. *Nano Lett.* **2011**, *11*, 5071−5078.

(16) Shao, Y.; Ding, F.; Xiao, J.; Zhang, J.; Xu, W.; Park, S.; Zhang, J.-G.; Wang, Y.; Liu, J. *Adv. Funct. Mater.* **2013**, *23*, 987−1004.

(17) Lee, J.-S.; Tai Kim, S.; Cao, R.; Choi, N.-S.; Liu, M.; Lee, K. T.; Cho, J. *Adv. Energy Mater.* **2011**, *1*, 34−50.

DOI: 10.1021/acs.nanolett.5b02432
Nano Lett. 2015, 15, 6149−6154

(18) Ota, H.; Sakata, Y.; Otake, Y.; Shima, K.; Ue, M.; Yamaki, J.-i. *J. Electrochem. Soc.* **2004**, *151*, A1778−A1788.
(19) Zhang, S. S. *J. Power Sources* **2006**, *162*, 1379−1394.
(20) Lu, Y.; Tu, Z.; Archer, L. A. *Nat. Mater.* **2014**, *13*, 961−969.
(21) Lu, Y.; Das, S. K.; Moganty, S. S.; Archer, L. A. *Adv. Mater.* **2012**, *24*, 4430−4435.
(22) Lu, Y.; Korf, K.; Kambe, Y.; Tu, Z.; Archer, L. A. *Angew. Chem., Int. Ed.* **2014**, *53*, 488−492.
(23) Ding, F.; Xu, W.; Graff, G. L.; Zhang, J.; Sushko, M. L.; Chen, X.; Shao, Y.; Engelhard, M. H.; Nie, Z.; Xiao, J.; Liu, X.; Sushko, P. V.; Liu, J.; Zhang, J.-G. *J. Am. Chem. Soc.* **2013**, *135*, 4450−4456.
(24) Zhang, Y.; Qian, J.; Xu, W.; Russell, S. M.; Chen, X.; Nasybulin, E.; Bhattacharya, P.; Engelhard, M. H.; Mei, D.; Cao, R.; Ding, F.; Cresce, A. V.; Xu, K.; Zhang, J.-G. *Nano Lett.* **2014**, *14*, 6889−6896.
(25) Sannier, L.; Bouchet, R.; Santinacci, L.; Grugeon, S.; Tarascon, J.-M. *J. Electrochem. Soc.* **2004**, *151*, A873−A879.
(26) Croce, F.; Appetecchi, G. B.; Persi, L.; Scrosati, B. *Nature* **1998**, *394*, 456−458.
(27) Murugan, R.; Thangadurai, V.; Weppner, W. *Angew. Chem., Int. Ed.* **2007**, *46*, 7778−7781.
(28) Kamaya, N.; Homma, K.; Yamakawa, Y.; Hirayama, M.; Kanno, R.; Yonemura, M.; Kamiyama, T.; Kato, Y.; Hama, S.; Kawamoto, K.; Mitsui, A. *Nat. Mater.* **2011**, *10*, 682−686.
(29) Bouchet, R.; Maria, S.; Meziane, R.; Aboulaich, A.; Lienafa, L.; Bonnet, J.-P.; Phan, T. N. T.; Bertin, D.; Gigmes, D.; Devaux, D.; Denoyel, R.; Armand, M. *Nat. Mater.* **2013**, *12*, 452−457.
(30) Zheng, G.; Lee, S. W.; Liang, Z.; Lee, H.-W.; Yan, K.; Yao, H.; Wang, H.; Li, W.; Chu, S.; Cui, Y. *Nat. Nanotechnol.* **2014**, *9*, 618−623.
(31) Yan, K.; Lee, H.-W.; Gao, T.; Zheng, G.; Yao, H.; Wang, H.; Lu, Z.; Zhou, Y.; Liang, Z.; Liu, Z.; Chu, S.; Cui, Y. *Nano Lett.* **2014**, *14*, 6016−6022.
(32) Arora, P.; Zhang, Z. *Chem. Rev.* **2004**, *104*, 4419−4462.
(33) Lee, H.; Yanilmaz, M.; Toprakci, O.; Fu, K.; Zhang, X. *Energy Environ. Sci.* **2014**, *7*, 3857−3886.
(34) Zhang, X.; Ji, L.; Toprakci, O.; Liang, Y.; Alcoutlabi, M. *Polym. Rev.* **2011**, *51*, 239−264.
(35) Wu, H.; Zhuo, D.; Kong, D.; Cui, Y. *Nat. Commun.* **2014**, *5*, 5193.
(36) Zhang, S. S.; Xu, K.; Jow, T. R. *J. Power Sources* **2005**, *140*, 361−364.
(37) Jung, Y. S.; Cavanagh, A. S.; Gedvilas, L.; Widjonarko, N. E.; Scott, I. D.; Lee, S.-H.; Kim, G.-H.; George, S. M.; Dillon, A. C. *Adv. Energy Mater.* **2012**, *2*, 1022−1027.
(38) Lee, S. H.; Harding, J. R.; Liu, D. S.; D'Arcy, J. M.; Shao-Horn, Y.; Hammond, P. T. *Chem. Mater.* **2014**, *26*, 2579−2585.
(39) Ryou, M.-H.; Lee, D. J.; Lee, J.-N.; Lee, Y. M.; Park, J.-K.; Choi, J. W. *Adv. Energy Mater.* **2012**, *2*, 645−650.
(40) Kang, S. M.; Ryou, M.-H.; Choi, J. W.; Lee, H. *Chem. Mater.* **2012**, *24*, 3481−3485.
(41) Lin, Y.; Connell, J. W. *Nanoscale* **2012**, *4*, 6908−6939.
(42) Maher, P.; Dean, C. R.; Young, A. F.; Taniguchi, T.; Watanabe, K.; Shepard, K. L.; Hone, J.; Kim, P. *Nat. Phys.* **2013**, *9*, 154−158.
(43) Dean, C. R.; Young, A. F.; Meric, I.; Lee, C.; Wang, L.; Sorgenfrei, S.; Watanabe, K.; Taniguchi, T.; Kim, P.; Shepard, K. L.; Hone, J. *Nat. Nanotechnol.* **2010**, *5*, 722−726.
(44) Zhu, H.; Li, Y.; Fang, Z.; Xu, J.; Cao, F.; Wan, J.; Preston, C.; Yang, B.; Hu, L. *ACS Nano* **2014**, *8*, 3606−13.
(45) Marsh, K. L.; Souliman, M.; Kaner, R. B. *Chem. Commun.* **2015**, *51*, 187−190.
(46) Lin, Y.; Williams, T. V.; Connell, J. W. *J. Phys. Chem. Lett.* **2010**, *1*, 277−283.
(47) Chazalviel, J. N. *Phys. Rev. A: At., Mol., Opt. Phys.* **1990**, *42*, 7355−7367.
(48) Howlett, P. C.; MacFarlane, D. R.; Hollenkamp, A. F. *Electrochem. Solid-State Lett.* **2004**, *7*, A97−A101.
(49) Kozen, A. C.; Lin, C.-F.; Pearse, A. J.; Schroeder, M. A.; Han, X.; Hu, L.; Lee, S.-B.; Rubloff, G. W.; Noked, M. *ACS Nano* **2015**, *9*, 5884−5892.

DOI: 10.1021/acs.nanolett.5b02432
Nano Lett. 2015, 15, 6149−6154